

## Addressing and imaging microring resonators with optical evanescent light

R. Quidant

*ICFO-Institut de Ciències Fotòniques, Jordi Girona 29, Nexus II, 08034 Barcelona, Spain  
and LPUB, UMR-CNRS 5027, 9 Avenue A. Savary, F-21078 Dijon, France*

J.-C. Weeber and A. Dereux

*LPUB, UMR-CNRS 5027, 9 Avenue A. Savary, F-21078 Dijon, France*

G. Lévêque and J. Weiner

*LCAR, UMR-CNRS 5589, Université Paul Sabatier, 31062 Toulouse, France*

C. Girard

*CEMES, UPR-CNRS 8011, 29 Rue Jeanne Marvig, BP4347, F-31055 Toulouse, France*

(Received 24 October 2003; published 12 February 2004)

We show that *optical evanescent light* can be used to simultaneously address and image microring resonators. The optical addressing function is based on control of the overlap between a three-dimensional evanescent light spot and a linear dielectric ridge connected to the resonator. When detected with a Photon Scanning Tunnelling Microscope (PSTM), the evanescent light tailing off the device provides precise optical images of the light distribution inside and around the resonator. The complete phenomenon has been calculated numerically using the three-dimensional Green Dyadic Method.

DOI: 10.1103/PhysRevB.69.081402

PACS number(s): 78.20.Bh, 07.79.Fc, 78.68.+m

Current theoretical and experimental work on integrated optics devices aims to solve the problem of light guiding and addressing microring resonators or cylindrical optical microcavities.<sup>1–6</sup> In addition to their fundamental interest for studies of cavity QED,<sup>7,8</sup> microstructures can be integrated on a single wafer and therefore display high-speed communications functions such as add-drop wavelength switching, and high-order, dense-wavelength filtering.<sup>2,4,5</sup> These structures exhibit high resonance quality factors, well-suited for low-threshold microlaser technology.<sup>9</sup> In these examples, the guiding light process is supported by localized electromagnetic modes that have been tailored by an ensemble of semiconductor or dielectric guiding structures, lithographically designed at the surface of a sample. In order to inject the light energy inside a bus waveguide, these modes are usually excited by a propagating light beam focused into one end of the guide.<sup>10</sup>

Recent experimental work, building on developments in near-field optics instrumentation, investigates an alternative proposal of remote optical addressing based on the control of optical evanescent waves in coplanar geometry.<sup>11</sup> A new class of subwavelength optical experiments, applying either the optical tunnel effect (OTE) or lower mode based transmission (LMBT),<sup>12</sup> shows promise in the control light transfer through bent or segmented structures integrated in coplanar geometry.

In this Communication, a similar but complementary approach investigates addressing microring resonators featuring: (a) transverse sizes ranging in the subwavelength domain (down to  $\sigma \approx 150 \times 250 \text{ nm}^2$ ) and (b) optical modes confined laterally within a width of about half of the incident wavelength. To handle the difficulty of coupling such tiny structures, the key idea is to use evanescent optical fields instead of conventional propagating laser beams. Such a state

of the incident field can be produced by focused Gaussian beams incident on the transparent substrate in such a way that they are totally reflected in the absence of any structure deposited on the substrate surface. Recently, the usefulness of this coupling mode was studied in various configurations by extensive numerical simulations based on the Green dyadic technique,<sup>11</sup> and then confirmed by several experiments.<sup>12</sup> Here, this technique addresses ( $\lambda_0 = 633 \text{ nm}$ ), a bus waveguide connected to a microring cavity. After launching light inside the bus, we measure the optical electric field distribution established inside the device by frustrating the electric near-field that tails off the upper sides of the  $\text{TiO}_2$  structures. This last step is achieved by raster scanning the tip of a Photon Scanning Tunneling Microscope (PSTM).<sup>13–15</sup> With an unprecedented imaging quality, the PSTM data reveal many details related to the structure of the light field inside the whole device (energy losses, light intensity distribution around the connection area, effective wavelength of the excited mode, etc.). Finally, a comparison between experiment and numerical simulation for an ideal microring resonator, reveals the role of surface imperfections in the building of the standing wave pattern inside the cavity.

The sample used in this work was fabricated by standard electron beam lithography and reactive ion etching. First, a 150 nm thick  $\text{TiO}_2$  layer was coated on a glass substrate (residual roughness 1 nm) by ion assisted deposition. This deposition technique produces a  $\text{TiO}_2$  layer with a residual roughness of 3 nm, sufficiently smooth for carrying out the optical measurements. In a second step, the electron beam patterning was performed by a JEOL 840-A operating at 20 keV energy on a single layer of polymethylmethacrylate (PMMA) resist (950 K molecular weight and 150 nm thickness). After development of the PMMA film, a nickel coating

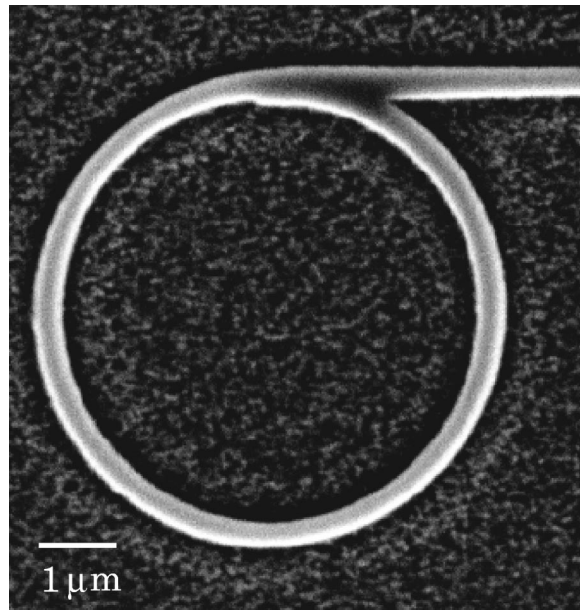


FIG. 1. Scanning electron microscopy picture of a  $\text{TiO}_2$  microring coupled with a linear waveguide ridge.

is evaporated onto the surface and the part in contact with the PMMA is lifted off by dissolution of the PMMA. The reactive ion etching is then performed in a GIR 300 Alcatel system. The etching process uses a  $\text{SF}_6$  (5/6)/Ar(1/6) equal flow rate gas mixture at a pressure of 0.015 mbar and a rf power of 40 W. The etching rate is typically 50 nm/min and the reactive ion etching parameters are optimized for steep sidewalls. Finally, the remaining Ni mask is removed in nitric acid solution. The resulting sample consists of a planar glass surface supporting a large number of microring resonators that all display the same geometrical parameters (6  $\mu\text{m}$  in diameter, 250 nm wide, and 150 nm high). Figure 1 presents a SEM picture of a typical microring resonator. The sample was then mounted on the prism of a PSTM.<sup>13–15</sup> In these near-field microscopes, a pointed tip is piezoelectrically driven to scan close to the sample surface so as to act as a local probe of the optical field in the near-field zone. The sharply elongated tips are obtained by pulling an optical fiber, subsequently coated with about 7 nm of Cr, resulting in no aperture at its very extremity. The PSTM tip scans at constant height. In this mode of operation, the signal detected by a PSTM is well-known to be related to the spatial distribution of the intensity of the optical electric field in the near-field zone ( $I_{\text{nf}}$ ).<sup>16</sup> This configuration of scanning near-field optical microscope has proved to be an efficient technique to characterize, in direct space and with subwavelength resolution, the optical properties of waveguides<sup>10,17–19</sup> or nanostructures integrated in coplanar geometry.<sup>20</sup> Specifically, the PSTM has turned out to be well-suited to map the propagation of light at the submicrometer scale.<sup>21,22</sup>

For our purpose, the specific feature of the PSTM setup is the incident field. Instead of the usual extended plane wave, we used a focused Gaussian beam which is totally reflected at the substrate interface. Some years ago a similar configuration was introduced by Dawson to trigger localized propagations of plasmon-polaritons at the surface of thin metallic

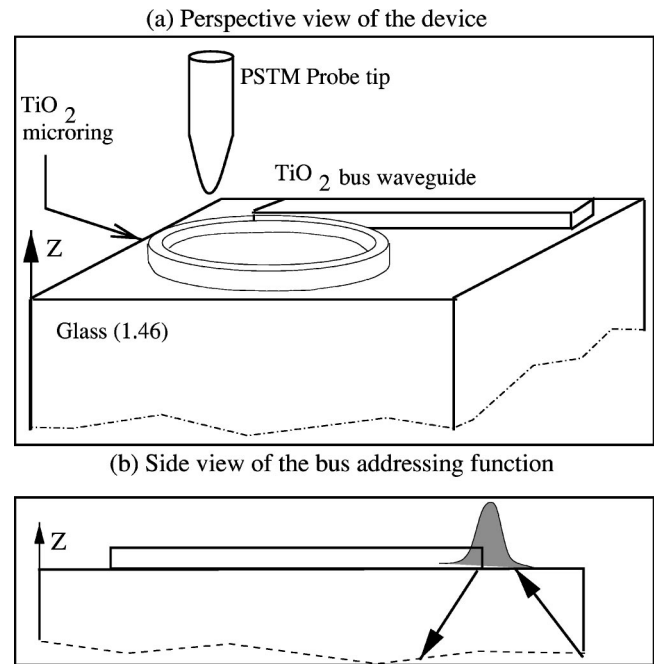


FIG. 2. Principle of simultaneous near-field optical addressing and PSTM imaging of a microring resonator. The adjacent bus waveguide is used to couple with the microring resonator. Index of refraction of the glass substrate is 1.46, of the  $\text{TiO}_2$  is 2.3.

layers.<sup>23</sup> In the present work, this local illumination is produced by a He–Ne laser (633 nm) injected in a lensed single mode fiber. The extremity of the fiber is oriented in such a way that the beam can be focused at the interface between the dielectric ridge and the glass substrate. We only considered the case of a transverse magnetic (TM) polarized incident beam where the coupling effect is expected to be more pronounced.

Figure 2 shows that the Gaussian beam is focused at the right extremity of the straight guide in such a way that the components of the incident wave vector parallel to the surface of the substrate align along the longitudinal axis of the guide. The tip is scanned at a constant height above the sample surface while monitoring the light intensity level. Successive images were recorded while moving the tip closer and closer to the surface of the sample. The last image, recorded at about 50 nm from the top surface of the lithographically designed structure, is presented in Fig. 3. This is the first image showing really what happens to light inside a microring resonator. A clear identification of working modes of such systems is only possible by using a near-field optical microscope because evanescent components lying at the surface of the guiding structures cannot propagate and must be converted by the tip into propagating light in order to be observed.

In spite of the subwavelength transverse dimensions of both linear and annular structures, the mode remains well-confined with some radiative loss localized around the microring. In this case, curvature loss can be attributed to energy escaping through the air–substrate interface. The full width at half maximum of the spatial distribution of the intensity of the mode along a transverse direction with respect

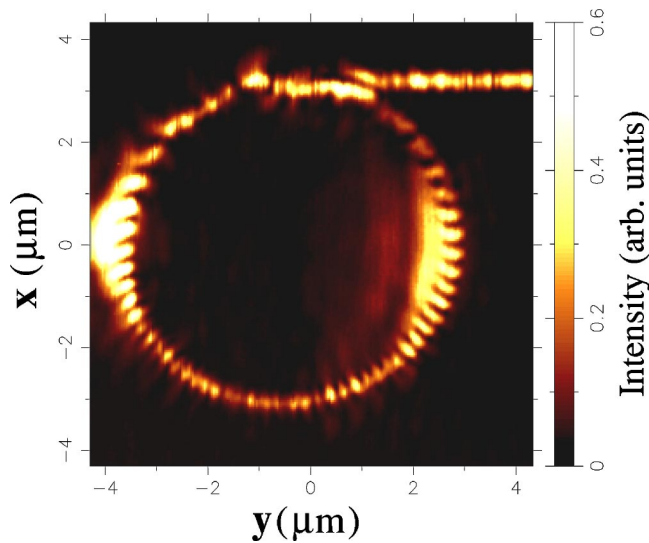


FIG. 3. (Color online) PSTM image recorded above the microring. The probe tip scans in plane parallel to the sample located at 50 nm from the  $\text{TiO}_2$  structures.

to the straight guide is found to be around 300 nm. It may be seen, that the light field established inside the microring displays a standing-wave pattern resulting from the interference of the incoming light in the ring with the light reflected back by the junction between the bus waveguide and the ring. Depending on its location inside the ring, the fringe pattern appears more and less fuzzy, due probably to residual roughness (estimated at  $\approx 15$  nm with AFM measurements) at the surface of the  $\text{TiO}_2$  structures. These surface imperfections can produce random scattering that locally degrade the expected ideal fringe pattern. However, the scattering by these imperfections cannot completely explain the two bright spots visible on the PSTM image at both sides of the ring circumference. These two spots are probably generated by forward scattering spots related to a direct illumination of the microring by a residual part of the incident field. This assumption is supported by the fact that the bright spots are created by the part of the microring perpendicular to the plane of incidence for which the scattering of the incident light is expected to be the largest. The existence of these forward scattering spots does not prevent the measurement on the PSTM image of the standing wave pattern periodicity observed over the microring. A closer examination of the data following a cross-cut along a circle segment located inside the microring (cf. Fig. 3) reveals a periodicity of 220 nm corresponding to an effective index of the guided mode of about 1.44.

In order to complete our experimental study, we have performed extensive numerical simulations based on the *localized dyadic Green function method*. Such *ab initio* investigations of the optical near-field distributions only require a specification of the frequency dependent dielectric constant and the precise shape of the lithographically designed structures. Consequently, they can stand alone, complement and even anticipate experimental studies. Under some circumstances it is possible with this method to perform computational experiments before effective realization. In this Communication, we have simulated the observed penetration of

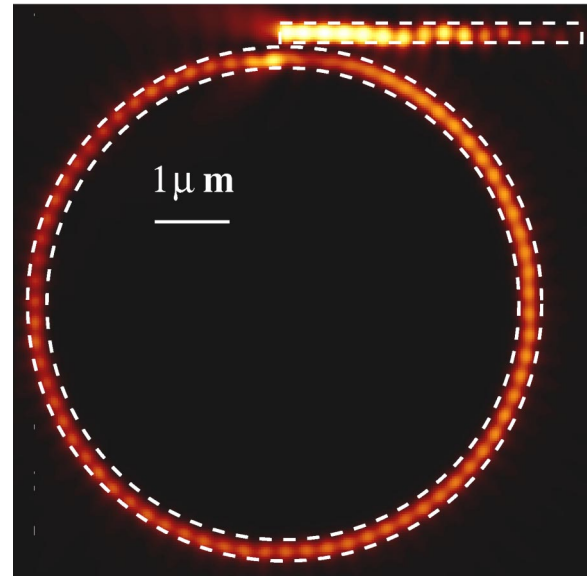


FIG. 4. (Color online) Map of the electric near-field intensity computed 50 nm over a  $4.0 \mu\text{m}$  long homogeneous waveguide coupled to a microring of  $6 \mu\text{m}$  diameter.

light inside a  $\text{TiO}_2$  bus ridge addressing a microring resonator of  $6 \mu\text{m}$  diameter by computing the electromagnetic near-field distribution in a plane parallel to the sample surface, when it is illuminated with an evanescent Gaussian beam. On the basis of the knowledge of the Green dyadic  $\mathcal{G}_{\text{ref}}(\mathbf{r}, \mathbf{r}', \omega)$ ,<sup>24</sup> which defines the response of a reference system (in our case, an air-glass interface), the method computes the electric field  $\mathbf{E}(\mathbf{r}, \omega)$  associated with the optical wave by solving numerically the discretization in direct space of the following integral equation:

$$\mathbf{E}(\mathbf{r}, \omega) = \mathbf{E}_0(\mathbf{r}, \omega) + \int_{\Omega} d\mathbf{r}' \mathcal{G}_{\text{ref}}(\mathbf{r}, \mathbf{r}', \omega) \cdot \chi(\mathbf{r}', \omega) \cdot \mathbf{E}(\mathbf{r}', \omega),$$

where the integral runs over the volume  $\Omega$  occupied by the device deposited on the surface and  $\chi(\mathbf{r}', \omega) = (\varepsilon - 1)/4\pi$ , where  $\varepsilon$  denotes the dielectric constant of  $\text{TiO}_2$ . In the case of a Gaussian beam incoming under the condition of total internal reflection, the calculation of the incident field  $\mathbf{E}_0(\mathbf{r}, \omega)$  is detailed in Refs. 11, 25. We repeated the computations of 11 for the parameters of the section of the  $\text{TiO}_2$  structures studied here but, in order to keep a reasonable calculation time, the length of the bus waveguide was reduced to  $4 \mu\text{m}$ . The modeling assumed perfect structures of  $\text{TiO}_2$  (optical index 2.3) supported by a half space filled of glass (optical index 1.46).

In Fig. 4, we present a map of the numerical output calculated in a plane located 50 nm over the sample. When examining this image, one can see that the light homogeneously fills out the ring core without significant radiative losses outside the device. Consequently, the radiative losses actually observed in the PSTM image Fig. 3 could be produced by residual surface roughness existing along the sides of the ring. According to the experimental map of Fig. 3, the period of the fringe pattern is found to be about 220 nm as

well. We note also that the intensity pattern inside the ring core is two times smaller than the intensity inside the bus waveguide. This means that the wavelength  $\lambda_0 = 633$  nm does not exactly correspond to a resonance of the physical ring structure. In both experimental and theoretical images, a single maximum occurring along the transverse directions of the structures, suggests that the light propagation inside the *dielectric structures of higher optical index* is supported by their lowest frequency modes. Except for a less pronounced fringe pattern of the field intensity, we notice a striking similarity between the measured field intensity, Fig. 3, and the numerical simulation, Fig. 4.

To summarize, the experiment described in this paper clearly demonstrates that *optical evanescent light* can be used to simultaneously address and image microring resonators or other integrated optics devices. When the transverse dimension of the microwaveguide is subwavelength, the

guiding process relies on the lowest frequency mode sustained by the device. Such a mode can be excited locally at the entry of a bus waveguide by focusing a totally reflected Gaussian beam and detected, in a subwavelength volume. We have thus shown that this nonstandard coupling technique is efficient to excite narrow waveguides and resonators in coplanar geometry. In agreement with theoretical predictions, PSTM images have revealed, in direct space, possible energy transfers inside a microring with a mode confined laterally within a width of about the half of the incident wavelength. These new kinds of near-field optical experiments could stimulate promising applications in the domain of integrated optics, especially for the design of more compact microring resonators.

We have benefited from the computing facilities provided by the massively parallel center CALMIP of Toulouse.

- 
- <sup>1</sup>B.E. Little, S.T. Chu, and H.A. Haus, *Opt. Lett.* **23**, 894 (1998).  
<sup>2</sup>B.E. Little, S.T. Chu, W. Pan, D. Ripin, T. Kaneko, Y. Kokubun, and E. Ippen, *IEEE Photonics Technol. Lett.* **11**, 215 (1999).  
<sup>3</sup>F.C. Blom, H. Kelderman, H.J.W.M. Hoeskstra, A. Driessen, Th.J.A. Popma, S.T. Chu, and B.E. Little, *Opt. Commun.* **167**, 77 (1999).  
<sup>4</sup>B.E. Little, S.T. Chu, J.V. Hryniewicz, and P.P. Absil, *Opt. Lett.* **25**, 344 (2000).  
<sup>5</sup>R. Grover, P.P. Absil, V. Van, J.V. Hryniewicz, B.E. Little, O. King, L.C. Calhoun, F.G. Johnson, and P.T. Ho, *Opt. Lett.* **26**, 506 (2001).  
<sup>6</sup>M.K. Chin and S.T. Ho, *J. Lightwave Technol.* **16**, 1433 (1998).  
<sup>7</sup>P. R. Berman, *Cavity Quantum Electrodynamics* (Academic, San Diego, 1994).  
<sup>8</sup>P. Munstermann, T. Fischer, P. Maunz, P.W.H. Pinkse, and G. Rempe, *Phys. Rev. Lett.* **84**, 4068 (2000).  
<sup>9</sup>P.L. Gourley, *Sci. Am.* **273**, 56 (1998).  
<sup>10</sup>M.L.M. Balistreri, D.J.W. Klunder, F.C. Blom, A. Driessen, J.P. Korterik, L. Kuipers, and N.F. van Hulst, *J. Opt. Soc. Am. B* **18**, 465 (2001).  
<sup>11</sup>J.C. Weeber, A. Dereux, Ch. Girard, G. Colas des Francs, J.R. Krenn, and J-P. Goudonnet, *Phys. Rev. E* **62**, 7381 (2000).  
<sup>12</sup>C. Girard, A. Dereux, R. Quidant, G. Colas des Francs, and J.C. Weeber, *Int. J. Nanosci.* **1**, 63 (2002).  
<sup>13</sup>R.C. Reddick, R.J. Warmack, and T.L. Ferrell, *Phys. Rev. B* **39**, 767 (1989).  
<sup>14</sup>D. Courjon, K. Sarayedine, and M. Spajer, *Opt. Commun.* **71**, 23 (1989).  
<sup>15</sup>N.F. van Hulst, N.P. de Boer, and B. Bölger, *J. Microsc.* **163**, 117 (1991).  
<sup>16</sup>J.C. Weeber, E. Bourillot, A. Dereux, J-P. Goudonnet, Y. Chen, and C. Girard, *Phys. Rev. Lett.* **77**, 5332 (1996).  
<sup>17</sup>A.G. Choo, H.E. Jackson, U. Thiel, G.N. De Brabander, and J.T. Boyd, *Appl. Phys. Lett.* **65**, 947 (1994).  
<sup>18</sup>M.L.M. Balistreri, J.P. Korterik, L. Kuipers, and N.F. van Hulst, *Appl. Phys. Lett.* **77**, 4092 (2000).  
<sup>19</sup>M.L.M. Balistreri, J.P. Korterik, L. Kuipers, and N.F. van Hulst, *Phys. Rev. Lett.* **85**, 294 (2000).  
<sup>20</sup>D. Mullin, M. Spajer, D. Courjon, F. Carcenac, and Y. Chen, *J. Appl. Phys.* **87**, 534 (2000).  
<sup>21</sup>M.L.M. Balistreri, H. Gersen, J.P. Korterik, L. Kuipers, and N.F. van Hulst, *Science* **294**, 1080 (2001).  
<sup>22</sup>R. Quidant, J.C. Weeber, A. Dereux, D. Peyrade, G. Colas des Francs, and Ch. Girard, *Phys. Rev. E* **64**, 066607 (2001).  
<sup>23</sup>P. Dawson, F. de Fornel, and J.P. Goudonnet, *Phys. Rev. Lett.* **72**, 2927 (1994).  
<sup>24</sup>A.A. Maradudin and D.L. Mills, *Phys. Rev. B* **11**, 1392 (1975).  
<sup>25</sup>F.I. Baida, D.V. Labeke, and J.M. Vigoureux, *Phys. Rev. B* **60**, 7812 (1999).